

## CHAPTER SEVENTY ONE

### COMBINED REFRACTION-DIFFRACTION CALCULATIONS WITH DIRECTIONAL WAVE SPECTRA

P. Gaillard

SOGREAH, Grenoble, France

#### ABSTRACT

A method of calculation of the combined effects of wave refraction, diffraction and reflection in harbours of arbitrary shape and non uniform water depth, subject to periodic or random waves is presented. Examples of application are given and practical aspects on the wave spectrum discretisation are considered.

#### INTRODUCTION

The study of wave disturbance within harbours at the design stage has for many years been considered in terms of harbour response to various isolated unidirectional periodic waves both in laboratory scale models and numerical models. With the increasing application of wave measurement techniques giving information on the directional wave spectrum, a need is now felt to account for the directional spreading of wave energy, as well as for its frequency-wise distribution, in the design of ocean and coastal structures.

Numerical methods applying either refraction calculations (Collins et al [3]) or diffraction calculations in constant water depth (Goda et al [4], Nagai [6]) to directionally distributed random waves have formerly been published. However, methods involving both refraction and diffraction effects are required for engineering studies.

This paper presents a method of calculation of the combined effects of wave diffraction, reflection and refraction in harbours of arbitrary shape and non uniform water depth, which applies equally to periodic waves and random waves, conforming to a given directional wave spectrum.

This method has been applied since 1977 in studies of harbour projects involving periodic waves as offshore boundary conditions. It has recently been extended to account for prescribed irregular wave characteristics at the model boundaries.

## METHOD APPLIED WITH PERIODIC WAVES OR SPECTRAL COMPONENTS

The area investigated at the harbour site is discretised into a set of connected basins with constant water depths, these generally being unequal and conforming to the sea-bed topography. Within each of these domains, the problem is dealt with by a boundary integral element method as described by Barailler and Gaillard [1], Biesel and Ranson [2]. The refraction effects due to the sea-bed configuration are taken into account at the common boundaries between connected basins.

The excitation of the harbour by a periodic incident wave of angular frequency  $\omega$  induces a steady state dynamic response of the same frequency. The water surface elevation  $\zeta$  and the velocity potential  $\phi$  are accordingly expressed in the form:

$$\begin{aligned}\zeta(x,y,t) &= \text{Re} \left\{ \bar{\zeta}(x,y) e^{-i\omega t} \right\} \\ \phi(x,y,z,t) &= \text{Re} \left\{ \bar{\phi}(x,y,z) e^{-i\omega t} \right\}\end{aligned}\quad (1)$$

The unknown complex function  $\bar{\zeta}$  is, within each basin of constant depth  $h$ , a solution of the Helmholtz equation:

$$\nabla^2 \bar{\zeta} + k^2 \bar{\zeta} = 0 \quad (2)$$

with:

$$\omega^2 = gk \tanh kh \quad (3)$$

The function  $\bar{\phi}$  can be derived from  $\bar{\zeta}$  by the formula:

$$\bar{\phi}(x,y,z) = -i \frac{g}{\omega} \bar{\zeta}(x,y) \frac{\cosh k(z+h)}{\cosh kh} \quad (4)$$

The solution of (2) is expressed in the form of the boundary integral:

$$\bar{\zeta}_0 = -\frac{i}{4} \int_{\Gamma} \frac{\partial \bar{\zeta}}{\partial n} G_2(OM) ds \quad (5)$$

where:

$\Gamma$  is the boundary of the basin considered

$\partial/\partial n$  is the normal derivative taken positive inwards

$G_2(OM)$  the second Green's function associated with an arbitrary internal point  $O$  and a boundary point  $M$ , cf. fig. 1a.

$G_0(OM)$  is the solution of (2), which has a vanishing normal derivative along  $\Gamma$  and a logarithmic behaviour in the vicinity of  $O$ . When the domain is a half-plane, this solution is:

$$G_0(OM) = 2 H_0^{(1)}(kr) \quad (6)$$

$$\bar{\zeta}_0 = -\frac{1}{2} \int_{\Gamma} \frac{\partial \bar{\zeta}}{\partial n} H_0^{(1)}(kr) ds \tag{7}$$

where  $H_0^{(1)}$  is the Hankel function of the first kind and order zero. This formula can be applied to an arbitrarily shaped domain D by considering the combination of solutions associated with a discrete set of half-planes including D and bounded by the tangent to different sections of the boundary  $\Gamma$ . The area under investigation has to be subdivided into several basins of convex shape when necessary.

Furthermore, the normal derivative of  $\bar{\zeta}$  involved in (7) should be related exclusively to the waves entering into the basin considered. These waves may include:

- incoming waves with known characteristics, either given as basic data or derived from preliminary refraction calculations between the open sea and the harbour site. The sections of boundary where this occurs are referred to as main entrances;
- waves with unknown characteristics ab initio, which come from other connected basins or which are reflected from harbour structures. The sections of boundary where this occurs are classified as secondary entrances.

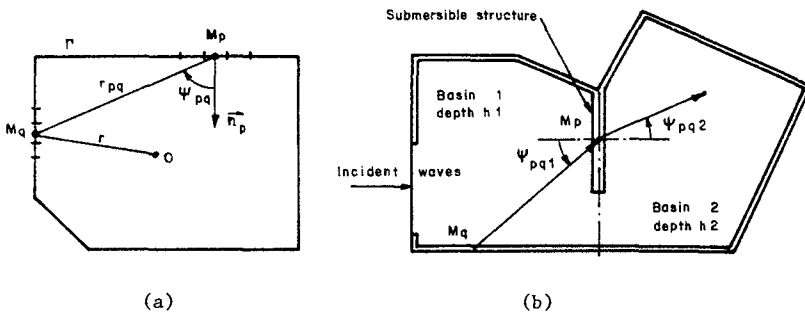


Fig. 1: Definition sketch

The method takes into account partial or total reflection from coastal structures and partial transmission when these are permeable or submersible, provided that the relevant coefficients are given. However, energy dissipation by bottom friction or wave breaking at locations other than these structures is not considered.

In the case of a reflective structure, the following boundary condition holds between the reflected (incoming) wave  $\bar{\zeta}_e$  and the incident (outgoing) wave  $\bar{\zeta}_s$ :

$$\bar{\zeta}_e = C_R \bar{\zeta}_s \tag{8}$$

$$\frac{\partial \bar{\zeta}}{\partial n} \bar{e} = - C_R \frac{\partial \bar{\zeta}}{\partial n} \bar{s} \quad (9)$$

$$\left( \frac{\partial \bar{\zeta}}{\partial n} \right)_p = - i \frac{k}{2} \int_{\Gamma} \left( \frac{\partial \bar{\zeta}}{\partial n} \right)_q H_1^{(1)}(kr_{pq}) \cos \Psi_{pq} ds \quad (10)$$

$$\Psi_{pq} = (\vec{n}_p, \vec{M}_p \vec{M}_q)$$

In the case of a permeable or submersible structure, the physical phenomenon can be complex because of the generation of harmonic wave components. As concerns the transmission of the fundamental component, the relationship between the outgoing wave in basin 1 and the incoming wave in basin 2, as shown in the figure 1b, is:

$$\bar{\zeta}_2 = C_T \bar{\zeta}_1 \quad (11)$$

$$\frac{\partial \bar{\zeta}}{\partial n} = - C_T \frac{\partial \bar{\zeta}}{\partial n} \quad \text{if } h_2 = h_1 \quad (12)$$

$$\left( \frac{\partial \bar{\zeta}}{\partial n} \right)_p = - M_{pq} \left( \frac{\partial \bar{\zeta}}{\partial n} \right)_q \quad \text{if } h_2 \neq h_1 \quad (13)$$

$$M_{pq} = \frac{k_2 \cos \Psi_{pq2}}{k_1 \cos \Psi_{pq1}} C_T \quad (14)$$

When the water depths in the adjacent basins are different, the direction of waves originating from a given boundary source,  $M_q$  varies according to Snell's law of refraction:

$$k_1 \sin \Psi_{pq1} = k_2 \sin \Psi_{pq2} \quad (15)$$

There is total reflection on the boundary if:

$$\Psi_{pq1} \geq \Psi_{1L} \quad \Psi_{1L} = \sin^{-1}(k_2/k_1) \quad (16)$$

This is observed for instance when waves propagating towards the shore encounter a navigation channel with an oblique incidence.

The complex parameters  $C_R$  and  $C_T$  have a modulus equal to the reflection or transmission coefficient of the structure and an argument equal to the phase lag introduced by the phenomenon considered. These parameters have to be derived from theoretical analysis or experimental investigations.

If the actual variation of water depth from one basin to another is gradual, i.e. with a sea-bed configuration of very mild slope which does not give rise to any appreciable wave reflection, the law of conservation of energy flux at the common boundary is applied.

$$\left| \bar{\zeta}_1 \right|^2 C_{g1} \cos \Psi_{pq1} = \left| \bar{\zeta}_2 \right|^2 C_{g2} \cos \Psi_{pq2} \quad (17)$$

This leads to the boundary condition (13) with:

$$M_{pq} = \frac{k_2}{k_1} \left[ \frac{C_{g1}}{C_{g2}} \frac{\cos \psi_{pq2}}{\cos \psi_{pq1}} \right]^{1/2} \quad (18)$$

The numerical calculation involves two steps:

- first, the solution of the system of equations resulting from the discretisation of the basin boundaries, the unknowns being the values of the normal derivative  $\partial \bar{\zeta} / \partial n$  in each basin at the centre of the boundary segments located on secondary entrances;
- then, the calculation of  $\bar{\zeta}$  in an arbitrary network of points by means of the discretised form of (7). This provides information on the spatial distribution of the local wave height  $2a$ , wave phase  $\theta$ , and diffraction coefficient  $K_d$  given by:

$$\bar{\zeta} = a e^{i\theta} \quad K_d = a/a_0 \quad (19)$$

where  $2a_0$  is the reference wave height given offshore or in the vicinity of the harbour entrance.

Additional information on the local wave direction  $\alpha$ , defined as the normal to the local constant phase line, and on the effective local wave number  $k_e$  is given by:

$$\frac{\partial \theta}{\partial x} = k_e \cos \alpha = \text{Im} \left\{ \frac{1}{\bar{\zeta}} \frac{\partial \bar{\zeta}}{\partial x} \right\} \quad (20)$$

$$\frac{\partial \theta}{\partial y} = k_e \sin \alpha = \text{Im} \left\{ \frac{1}{\bar{\zeta}} \frac{\partial \bar{\zeta}}{\partial y} \right\}$$

$$\left\{ \frac{\partial \bar{\zeta}}{\partial x}, \frac{\partial \bar{\zeta}}{\partial y} \right\} = -i \frac{k}{2} \int_{\Gamma} \frac{\partial \bar{\zeta}}{\partial n} H_1^{(1)}(kr) \left\{ \cos \mu, \sin \mu \right\} ds \quad (21)$$

$$\mu = (\vec{OX}, \vec{OM})$$

#### METHOD APPLIED WITH RANDOM WAVES

If the wave disturbance to be considered within the harbour results from random waves conforming to a given directional spectrum offshore, this spectrum is discretised into a finite set of directional and frequency-wise components. The harbour response to the excitation by each spectral component is calculated by the procedure described in the preceding section. This calculation gives:

- the diffraction coefficient  $K_d$  as a function of wave frequency  $f$ , initial wave direction  $\alpha_0$  and wave height  $a_0$ ; if the reflection and transmission coefficients of the structures involved in the study are considered as independent of the incident wave height,  $K_d$  will be independent of  $a_0$ , since the method is based on linear theory;

- the correspondence between the local wave direction  $\alpha$  and the initial direction  $\alpha_o$  of the spectral component.

From these results, it is possible to derive the local directional spectrum and frequency spectrum at any selected point P, by means of the following expressions:

$$S(f, \alpha, P) = S_o(f, \alpha_o) K_p^2 \quad K_p^2 = \frac{C_{go} C_o}{C_{gp} C_p} \quad (22)$$

$$S(f, P) = \int_0^{2\pi} S_o(f, \alpha_o) [K_d(f, \alpha_o, P)]^2 d\alpha_o \quad (23)$$

where:

$S_o(f, \alpha_o)$  is the reference wave spectrum

$C_o, C_{go}$  are respectively the phase and group velocities at the location where the reference wave spectrum is specified

$C_p, C_{gp}$  are the phase and group velocities at point P

$K_d$  and  $K_p$  are theoretically related by:

$$K_d^2 = K_p^2 \frac{\partial \alpha}{\partial \alpha_o} \quad (24)$$

The spatial distribution within the harbour of various overall spectral properties can be derived from the spectral moments:

$$M_j = \int_0^\infty df \int_0^{2\pi} f^j S_o(f, \alpha_o) K_d^2 d\alpha_o \quad (25)$$

$$M_{pq} = \int_0^\infty df \int_0^{2\pi} k^{p+q} \cos^p \alpha \cos^q \alpha S_o(f, \alpha_o) K_d^2 d\alpha_o \quad (26)$$

The following spectral parameters are considered in the applications of the method which are presented here: the significant wave height  $H_s$ , the mean zero-upcrossing wave period  $T_m$ , the mean wave direction  $\theta_m$  and the mean spreading angle  $\theta_s$ , as defined by Goda, Miura and Kato [5]. These parameters are defined by:

$$H_s = 4 \sqrt{M_o} \quad (27)$$

$$T_m = (M_o/M_2)^{1/2} \quad (28)$$

$$\theta_m = \tan^{-1} (M_{o1}/M_{1o}) \quad (29)$$

$$\theta_s = \tan^{-1} \left\{ \frac{\sqrt{M_{o0} (M_{o1}^2 M_{2o} - 2M_{1o} M_{o1} M_{11} + M_{1o}^2 M_{o2})}}{M_{o1}^2 + M_{1o}^2} \right\} \quad (30)$$

The parameters associated with the reference wave spectrum are represented by  $H_{so}, T_{mo}, \theta_{mo}, \theta_{so}$ .

## EXAMPLES OF APPLICATION

Several examples of application of the above method to complex harbour layouts with periodic and random waves are presented here. Besides, practical aspects on the wave spectrum discretisation techniques are considered in the case of a breakwater gap.

### Comparison with experimental data

Figure 2 shows the results of a comparative study of the wave disturbance within a harbour performed with a numerical model based on the above method and with a laboratory scale model at a scale of 1/150. The water depth ranges approximately between 31 m at the offshore boundary and 6 m in the nearshore zone of the harbour, and 24 diffraction basins were considered in the numerical model.

The results obtained for 12 s periodic waves are shown in the form of curves of constant relative wave-height, the latter being expressed in percentage of the reference wave-height offshore. The local wave direction, calculated by means of (20) (21), is also shown in figure 2b. A similar wave-height distribution is observed in both models.

### Harbour access channel effect on wave propagation

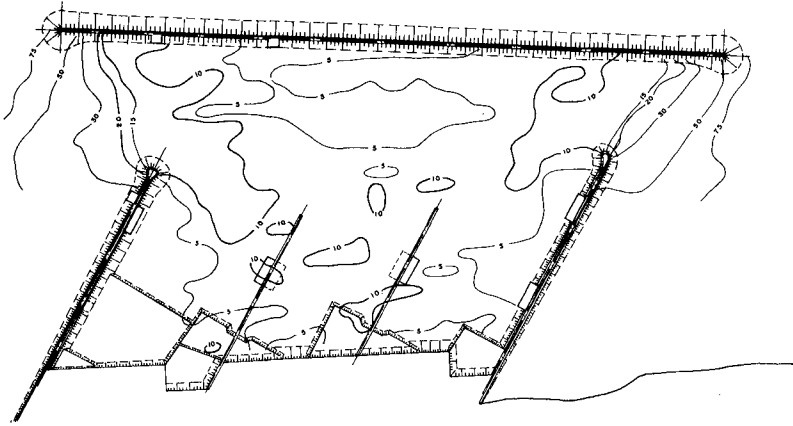
The second example is an application of the numerical method to the study of the impact of a harbour extension scheme on the wave disturbance in Fos harbour (France). This study, performed at the request of the Marseilles Port Authority, is illustrative of the effect of harbour access channels on wave propagation.

Figure 3 shows the area investigated, the location of the harbour entrance channel being indicated by dashed lines. The results obtained for wave periods of 6 and 8 seconds are shown respectively in figure 3a and b, with the same presentation as in figure 2b. An enlarged view of the wave height and wave direction distributions in the harbour area is shown at the left hand side of the figure. A smaller mesh size of the calculation network has been used for this purpose.

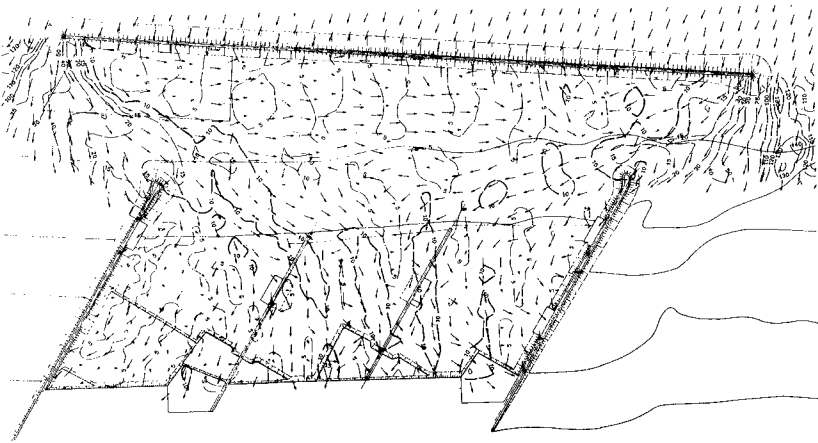
This figure shows a marked effect of the wave period on the wave pattern. The reflection of the incoming waves on the outer side of the harbour access channel is observed with the higher period and this produces a favourable sheltering effect in the harbour area.

### Wave spectrum discretisation techniques

In order to study the influence of the wave spectrum discretisation technique on the accuracy of results, numerical calculations have been done in the case of a breakwater gap in constant water depth with directional wave spectra representative of wind waves and swell respectively.



(a)



(b)

Fig. 2: Comparison of the wave-height distributions in a harbour obtained respectively with a laboratory scale model (a) and a numerical model (b) for 12 s periodic waves. In the latter model, the local wave direction is indicated by arrows.

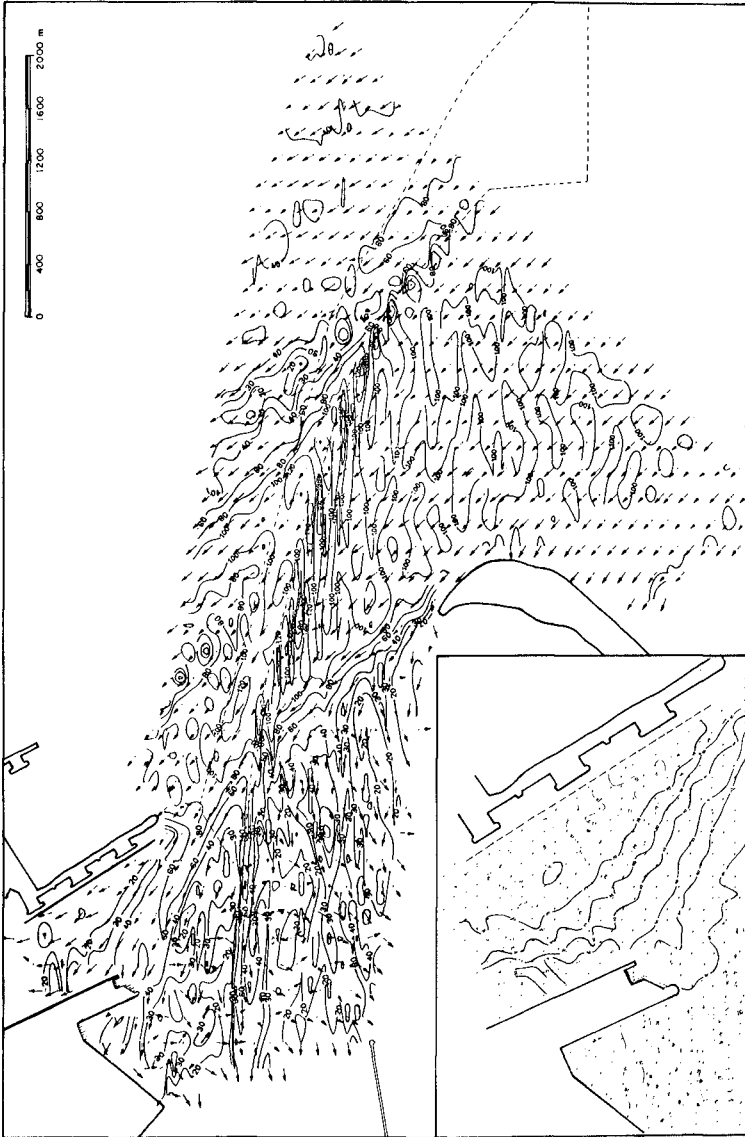


Fig. 3a: Wave-height and wave direction obtained with a numerical model of Fos harbour for waves of period  $T = 6$  s.

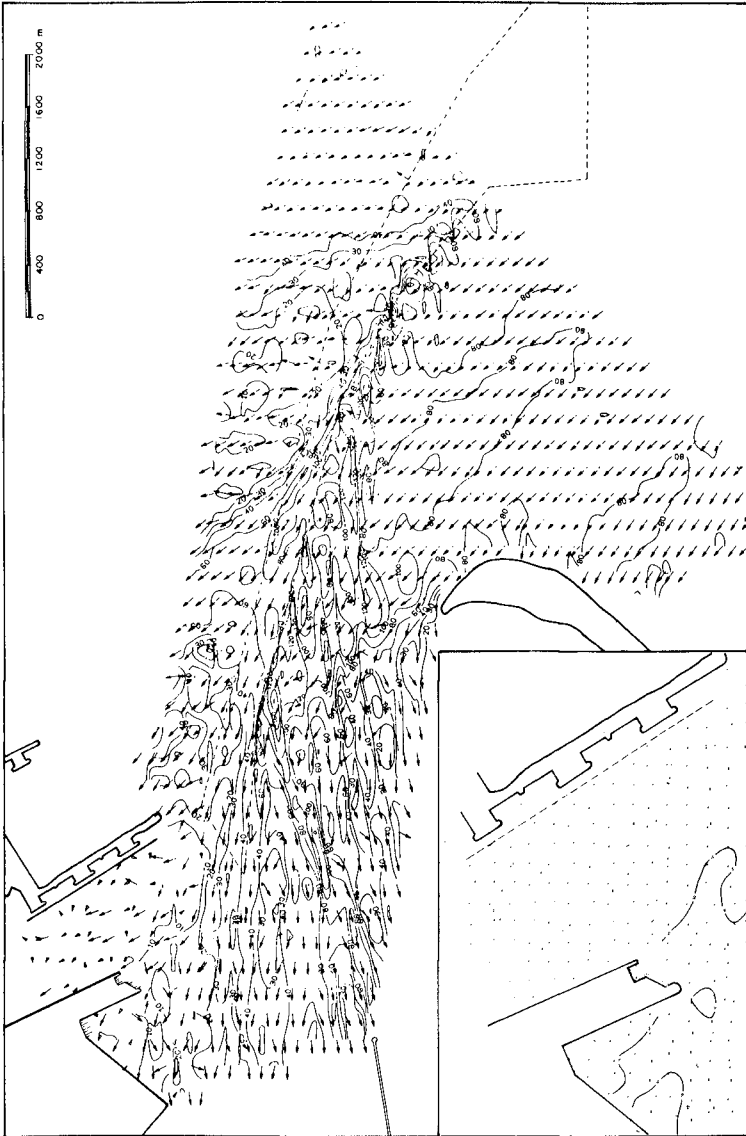


Fig. 3b: Wave-height and wave direction obtained with a numerical model of Fos harbour for waves of period  $T = 8$  s.

The incident wave spectra were chosen of the form proposed by Goda et al [4] :

$$S_o(f, \alpha_o) = \bar{S}_o(f) \cdot D(f, \alpha_o) \quad (31)$$

$$\bar{S}_o(f) = 0.312 H_s^2 T_p^{-4} f^{-5} \exp \left[ -\frac{5}{4} (T_p f)^{-4} \right] \quad (32)$$

$$D(f, \alpha_o) = C \left[ \cos \frac{1}{2} (\alpha_o - \theta_{mo}) \right]^{2s} \quad (33)$$

$$s = \begin{cases} s_{\max} (f/f_p)^5 & f \leq f_p \\ s_{\max} (f/f_p)^{-2.5} & f > f_p \end{cases} \quad (34)$$

where:

$T_p$  and  $f_p$  are the period and frequency of the spectral peak

$C$  is a normalisation constant.

In the example considered, the gap-width to wave length ratio corresponding to the spectral peak is approximately  $B/L_p = 1.81$ .

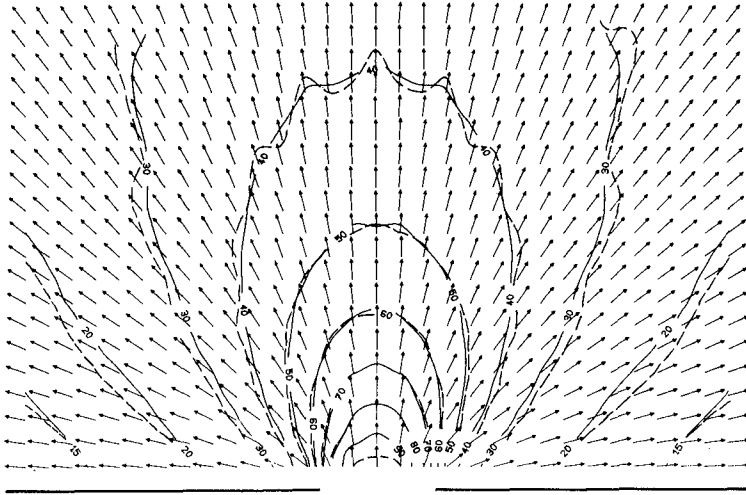
The results of two of the discretisation techniques implemented are reported here:

- The first one consists in a uniform allocation of wave energy to all frequency bands, this energy being lumped up at frequencies chosen in order to conserve the mean period defined by (28). The angular discretisation is done with a constant interval  $\Delta \alpha_o$  in a range of  $\pm \pi/2$  around the mean direction of the spectrum.
- The second technique is the same in the frequency domain. The angular discretisation is done with a constant interval, but the total range is reduced, the actual energy located beyond this range being allocated to the extreme angular components when this energy is lower than a given threshold value.

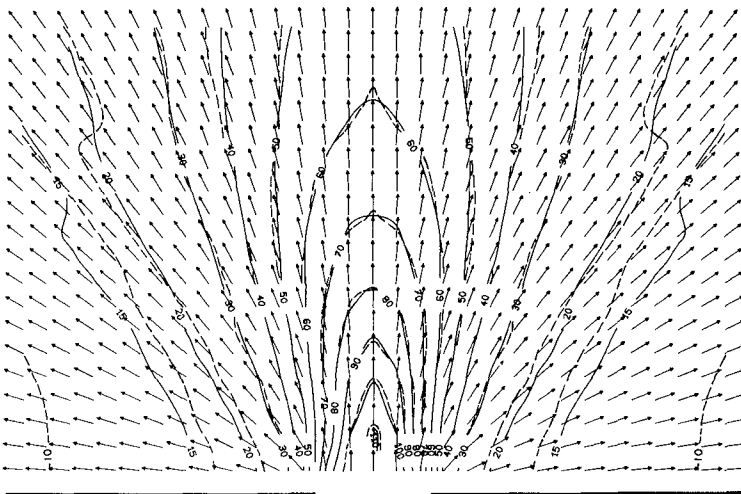
Figure 4 shows the distributions of the relative significant wave height  $H/H_{so}$  for the wave spectra corresponding respectively to  $s_{\max} = 10^0$  and 75. The full lines show the wave-height distribution resulting from the first technique with 204 spectral components, distributed in 12 frequency intervals. The dashed lines result from the second technique, which leads to the computation of 70 and 34 spectral components respectively for the broad and narrow spectra, with 6 frequency intervals. A good agreement of the results is found.

As concerns the mean wave direction  $\theta_m$ , indicated by arrows in figure 4, there is no discernible difference between the two techniques.

Figure 5 shows the distribution of the relative mean wave period  $T/T_m$  for the broad spectrum in the form of level curves. The results obtained with the first and second discretisation techniques are shown on the left and right hand sides of the gap centre-line respectively.



(a)



(b)

Fig. 4: Wave-height and wave direction behind a breakwater gap of relative width  $B/L = 1.83$  for random waves with: (a)  $s = 10$  (b)  $s = 75$ . The solid and dashed lines are related to the first and second discretisation techniques.

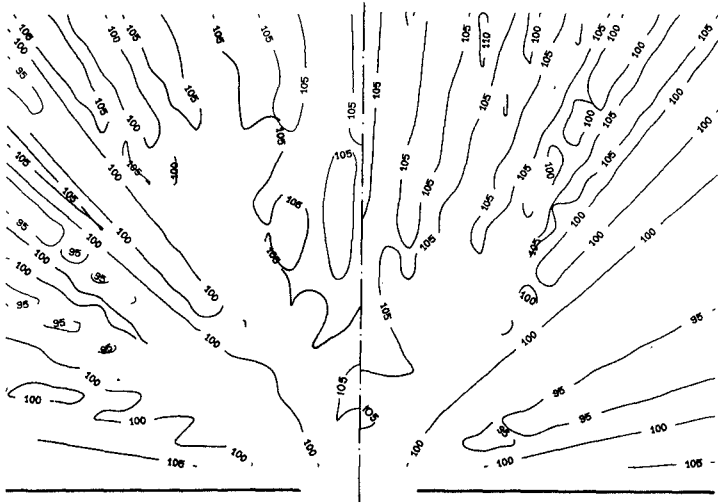


Fig. 5: Distribution of the mean wave period  $T_m/T_{m0}$  behind the breakwater gap for a directional wave spectrum with  $s = 10$ . See also legend of fig. 6.

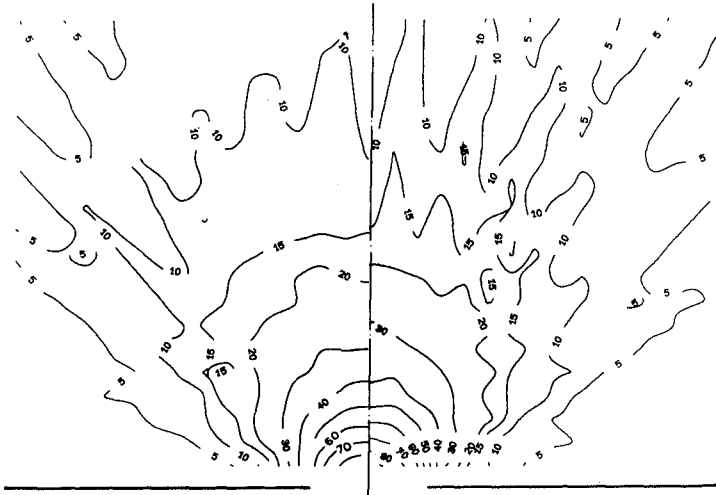


Fig. 6: Distribution of the mean spreading angle  $\theta/\theta_0$  for the same wave spectrum. LHS and RHS show the results of the first and second discretisation techniques (204 and 70 spectral components respectively).

Figure 6 shows the distribution of the ratio  $\theta_s/\theta_{s_0}$  for the same case with a similar presentation.

Differences due to the discretisation technique are more pronounced with the mean wave period and the mean spreading angle than with the significant wave height distribution, although the results are of the same order of magnitude. This sensitivity to discretisation is connected with the presence of higher moments of the wave spectrum in the expressions used for calculating these parameters.

#### Study of a complex harbour layout with random waves

Figures 7 and 8 give an example of study of the wave disturbance in a harbour of complex shape with random wave characteristics given as boundary conditions. In this case, the reference frequency spectrum is of the Jonswap type and the angular dispersion function is of the form (33) (34) with  $s_{\max} = 50$ . This relatively narrow spectrum is discretised into 39 spectral components, distributed over 5 frequency bands, by the second technique just described.

Figure 7a shows the spatial distribution of the diffraction coefficient  $K_d$  associated with one of the spectral components considered, in the form of curves of constant  $K_d$  values. The local wave direction associated with this period is indicated by arrows.

Figure 7b shows the distribution of the relative significant wave height  $H/H_{s_0}$  in the form of level curves and arrows indicate the local mean wave direction defined by equation (29).

Figure 8a shows the distribution of the relative mean wave period  $T_m/T_{m_0}$ , as defined by equation (28) and figure 8b the distribution of the relative mean spreading angle  $\theta_s/\theta_{s_0}$ , defined by equation (30). In this particular case, the wave reflection on the harbour structures tends to increase the angular spread of the locally observed wave spectrum and this effect predominates over the adverse effect of wave diffraction in many parts of the harbour.

#### CONCLUSION

The method described provides an interesting means of evaluation of wave disturbance in harbour projects, in terms of wave spectral properties. The numerical calculations confirm the conclusion of other authors that the directional spreading of wave spectra is an important characteristic to account for in such studies, if sufficient information is available on the local wave climate.

The second wave spectrum discretisation technique presented here is recommended for selecting the spectral components to account for in the calculations. The number of components needed depends on the type of input wave spectrum and on the wave parameters required.

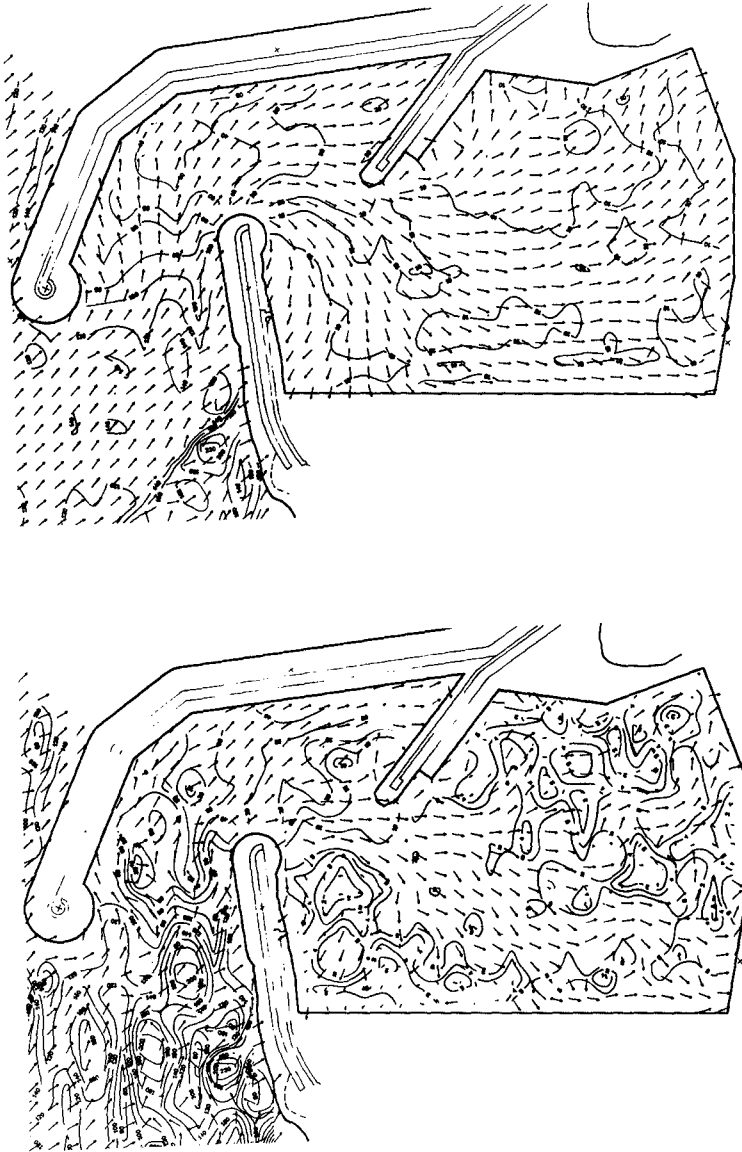


Fig. 7: Spatial distribution of: (a) coefficient  $K_d$  and wave direction  $\alpha$  for one spectral component, (b) significant wave height  $H_s/H_{s0}$  and mean wave direction  $\theta_m$  in a harbour of complex shape.

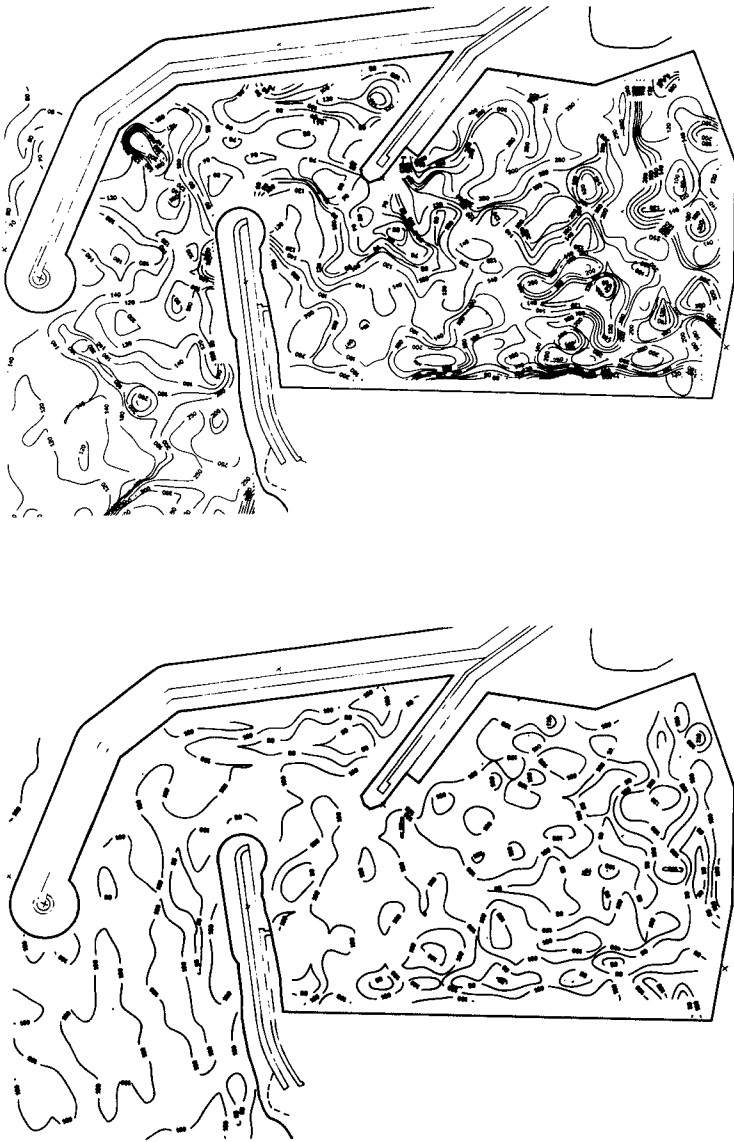


Fig. 8: Spatial distribution of (a) mean wave period  $T_m/T_{m0}$ , (b) mean dispersion angle  $\theta_s/\theta_{s0}$  in the harbour of figure 7.

The sensitivity analysis performed shows that the significant wave-height and mean wave direction are much less sensitive to the spectrum discretisation than the mean wave period and the mean spreading angle.

In practical applications, a careful choice of the reference directional wave spectrum is necessary, because of the marked influence of the angular distribution of energy on the wave pattern in sheltered areas and on the computer time required for these calculations.

#### REFERENCES

- [1] L. Barailler and P. Gaillard, 1964: Exemples de réalisation de modèles mathématiques à Sogreah pour des études de propagation de houle. Proc. 9th Coastal Engineering Conf., Lisbon, pp. 41-54.
- [2] F. Biesel and B. Ranson, 1961: Calculs de diffraction de la houle. IAHR Conference, Dubrovnik, pp. 688-699.
- [3] J.I. Collins, W.L. Chiang and F. Wu, 1981: Refraction of directional spectra. Proc. Conference on directional wave spectra applications, Berkeley, ASCE, pp. 251-268.
- [4] Y. Goda, T. Takayama and Y. Suzuki, 1978: Diffraction diagrams for directional random waves. Proc. 16th Coastal Engineering Conf., Hamburg, pp. 628-650.
- [5] Y. Goda, K. Miura and K. Kato, 1981: On-board analysis of mean wave direction with discus buoy. Int. Conf. on wave and wind directionality, Paris, Editions Technip, pp. 339-359.
- [6] K. Nagai, 1972: Diffraction of the irregular sea due to breakwaters. Coastal Engineering in Japan, JSCE, vol. 15 pp. 59-67.